Nano-Newton Transverse Force Sensor Using a Vertical GaN Nanowire based on the Piezotronic Effect

Yu Sheng Zhou, Ronan Hinchet, Ya Yang, Gustavo Ardila, Rudeesun Songmuang, Fang Zhang, Yan Zhang, Weihua Han, Ken Pradel, Laurent Montès, Mireille Mouis, and Zhong Lin Wang**

Semiconductor nanowires (NWs) have been researched as the building blocks for various nanosensors and devices, such as strain sensors,[1,2] photodetectors,[3] biosensors,[4] and gas sensors.[5] In recent years, wurtzite semiconductor NWs, such as ZnO, have been extensively investigated due to their piezoelectric properties.[6] With metal-semiconductor Schottky junctions, the electric transport through a NW can be modulated through external strain due to the piezotronic effect, using the polarization induced electric potential to tune the charge-carrier generation, transport, separation or recombination at a metal-semiconductor interface or a p-n junction.[6] The piezotronic effect has been used for fabricating various functional devices such as strain sensors,[1] piezoelectric switches,[7] electromechanical memory,[8] and strain-gated logic nanodevices.[9] The aforementioned devices are based on axial strain (or tensile strain) applied to a NW. However, for the sensing of transverse forces, the piezoresistive effect is minimized because one side of the nanowire is under compressive strain and the other side is under tensile strain. Fei et al. have demonstrated a force trigger using a piezotronic transistor at the root of a ZnO nanowire.[10]

In this paper, we explore the piezotronic effect in a GaN nanowire under a transverse force. The force was applied by bending the end of a single NW using an atomic force microscope (AFM) tip. Our results show that GaN NWs can be used to transduce a shear/bending force into a dramatic current change through the NW due to the piezotronic effect. Owing to the local piezopotential generated by the applied force, the barrier height of the Schottky contact between the GaN NW and the platinum AFM tip can be modulated. Using this transduction mechanism, the transverse force can be correlated to the natural logarithm of the current. Our results indicate that the force sensitivity is about 1.24 ± 0.13 ln(A)/nN, and a force resolution better than 16 nN is demonstrated. The nN sensitivity of GaN NWs shows the potential for piezoelectric semiconductor NWs to act as the main building blocks for micro-/nanometer-sized force sensor arrays and high spatial resolution artificial skin.

The n-type Si doped GaN NW array was synthesized by plasma assisted molecular beam epitaxy (MBE) on n-type Si (111) substrates.[11] The Si cell temperature used for n-type doping was found to yield an electron concentration of ≈2–5 × 10^{19} cm^{-3} in epitaxially grown bulk GaN, as determined by Hall-effect measurements. **Figure 1**a shows that the NWs are vertically aligned with a uniform length of about 1.5 μm. The low magnification transmission electron microscopy (TEM) image (Figure 1b) suggests that the NW diameter is about 60 nm. A corresponding high resolution TEM (HRTEM) image and selected area electron diffraction pattern (SAED) show that the as-grown GaN NWs are single crystalline with a wurtzite structure, and a growth direction of <0001> (Figure 1c).

In order to simulate transverse force conditions, we applied a bending force to the free end of a single GaN NW using an AFM, as illustrated in **Figure 2**a. To precisely position the AFM tip on the side of a single NW, we used the following procedure: Firstly the NW array sample was cleaved and tilted 90°. Then, a tapping mode image of the edge of the sample was taken (Figure 2b). Lastly, the AFM tip was moved to the free end of a single NW using the AFM's closed loop piezo scanner.[12]

In order to characterize the electric transport property under different transverse forces, three steps were applied to the experiments, as shown in Figure 2c. In the first step, the tip was engaged onto the free end of the NW with a preset force. The top curve in Figure 2c shows the applied force during the whole process. The applied force was increased by further deflecting the AFM cantilever. Secondly, after the applied force reached a preset value, the force remained constant during the dwell stage and the electrical measurements were initiated. In this stage, a sweeping bias between –2 V and +2 V was applied between the NW and the tip as shown in the middle curve in Figure 2c. The bottom curve is the current response to the applied bias. After the *I–V* measurements were performed, the AFM tip was retracted from the NW. During both the force exertion stage and *I–V* measurement stages, any unstable conditions such as the tip sliding over the NW, or external disturbances such as mechanical drifting, can be easily differentiated

Y. S. Zhou, Dr. Y. Yang, F. Zhang, Prof. Y. Zhang, Prof. W. H. Han, K. Pradel, Prof. Z. L. Wang
School of Materials Science and Engineering
Georgia Institute of Technology
Atlanta, GA 30332-0245, USA
E-mail: zlwang@gatech.edu
R. Hinchet, Dr. G. Ardila, Dr. L. Montès, Dr. M. Mouis
IMEP-LAHC, MINATEC, 38016 Grenoble, France
E-mail: ardilarg@minatec.inpg.fr
Dr. R. Songmuang
CEA-CNRS Group Nanophysics and Semiconductors
Institute Néel, 38054 Grenoble, France
Prof. Z. L. Wang
Beijing Institute of Nanoenergy and Nanosystems
Chinese Academy of Sciences, Beijing, China.

DOI: 10.1002/adma.201203263

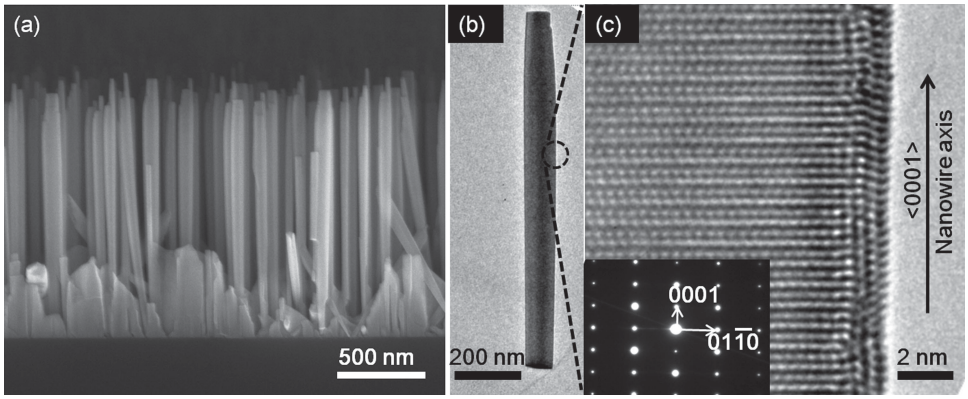

Figure 1. a) SEM side view of the vertically aligned GaN NW array grown on a Si substrate. b) Low magnification TEM image of a GaN NW. c) High resolution TEM image and corresponding SAED pattern (inset).

by monitoring the continuity of the force as a function of time in the extend and dwell stage (details described in the Supporting Information).

Prior to the *I–V* measurements, potential measurements were performed. We used the method described by Xu et al.[12] to measure the piezoelectric potential generated by the GaN NWs. As presented on **Figure 3**a, we used a conductive Pt coated AFM tip to apply a transverse force at the free end of a vertically grown GaN NW producing a downward deformation. The top side of the NW is under tension while the down side is under compression. This strain generates a piezoelectric potential in the GaN NW. As presented in Figure 3b, a positive piezoelectric potential was detected between the AFM tip and the free end of the GaN NW. This magnitude of the piezoelectric potential is proportional to the force for the small applied forces in the experiments (200 to 1000 nN).

In the subsequent *I–V* measurements, there were two metal-semiconductor contacts. One was the contact between the Pt coated AFM tip and GaN NW, while the other was between the silver electrode and the Si wafer. The work functions of the two metals are higher than the corresponding semiconductors' electron affinities. As a result, both contacts are Schottky contacts with different barrier heights. The Schottky barrier height (SBH, Φ_B) of the Ag-Si contact is assumed to be much lower than that of the Pt-GaN one, given that the work functions of Pt and Ag are 5.65 and 4.26 eV,[13] respectively, and the electron affinities of GaN and Si are 4.1[14] and 4.05 eV, respectively. The conduction band discontinuity between GaN NW and Si is negligible due to the 0.05 eV difference in electron affinity and assuming a small difference in the doping concentration.[11] The schematic energy band diagram is shown in **Figure 4**a.

According to the piezotronic theory,[15] a positive local piezopotential would lower the SBH, as illustrated in Figure 4b, subsequently increasing the current flow through the NW. Due to the Ag-Si contact's opposite rectifying direction, the current flow from the Pt to the NW, defined as positive here, would be

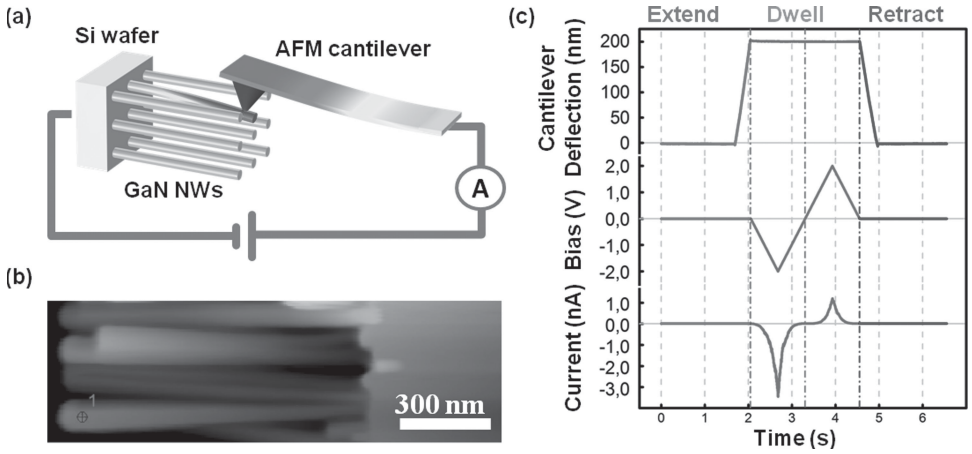

Figure 2. a) Schematic of the AFM experimental setup. b) AFM image of a 90° tilted GaN NW ensemble. The red mark on one of the NWs indicates the location of the AFM tip during the electrical measurement. c) Illustration of the experiment process: from top to bottom, the cantilever deflection that is proportional to the applied force on the GaN NW; a bias applied between the AFM tip and the sample; and the corresponding detected current.

Adv. Mater. **2012**,
DOI: 10.1002/adma.201203263

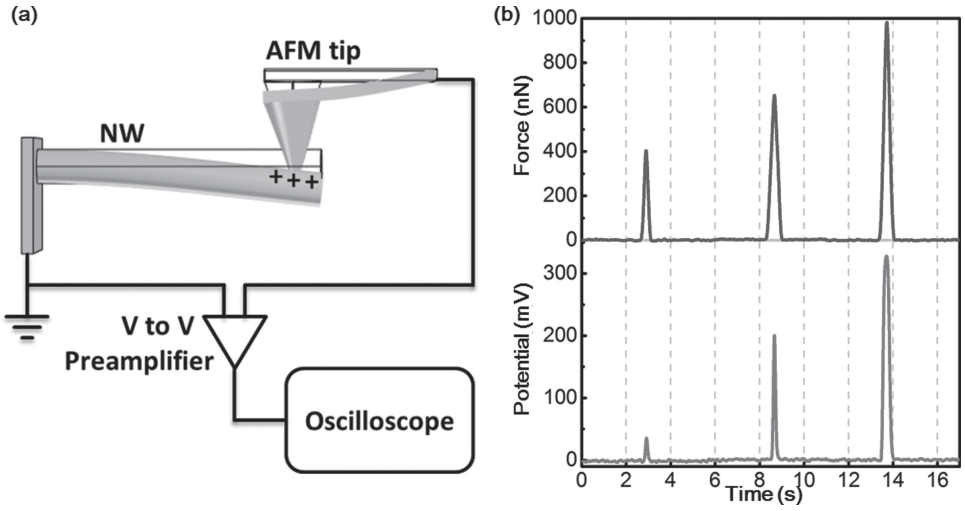

Figure 3. a) Schematic of the NW displacement and the experiment setup used for measuring the piezoelectric potential generated by the GaN NWs. b) AFM measurements of the piezoelectric potential generated by a GaN NW under different bending forces.

largely limited by the reversely biased Ag-Si Schottky contact, while the current in the reverse direction, defined as negative here, will be dominated by the Pt-GaN Schottky contact. Therefore, by monitoring the negative current, a change in SBH of Pt-GaN contact can be derived, and the applied force can be quantified.

Experimental results are shown in Figure 4c,d. The current under negative bias dramatically increased as the force increased from 104 to 312 nN. This asymmetric current change is mainly due to the piezotronic effect as the piezopotential reduces the SBH between the Pt coated AFM tip and the GaN NW. Under positive bias, the current was largely limited by

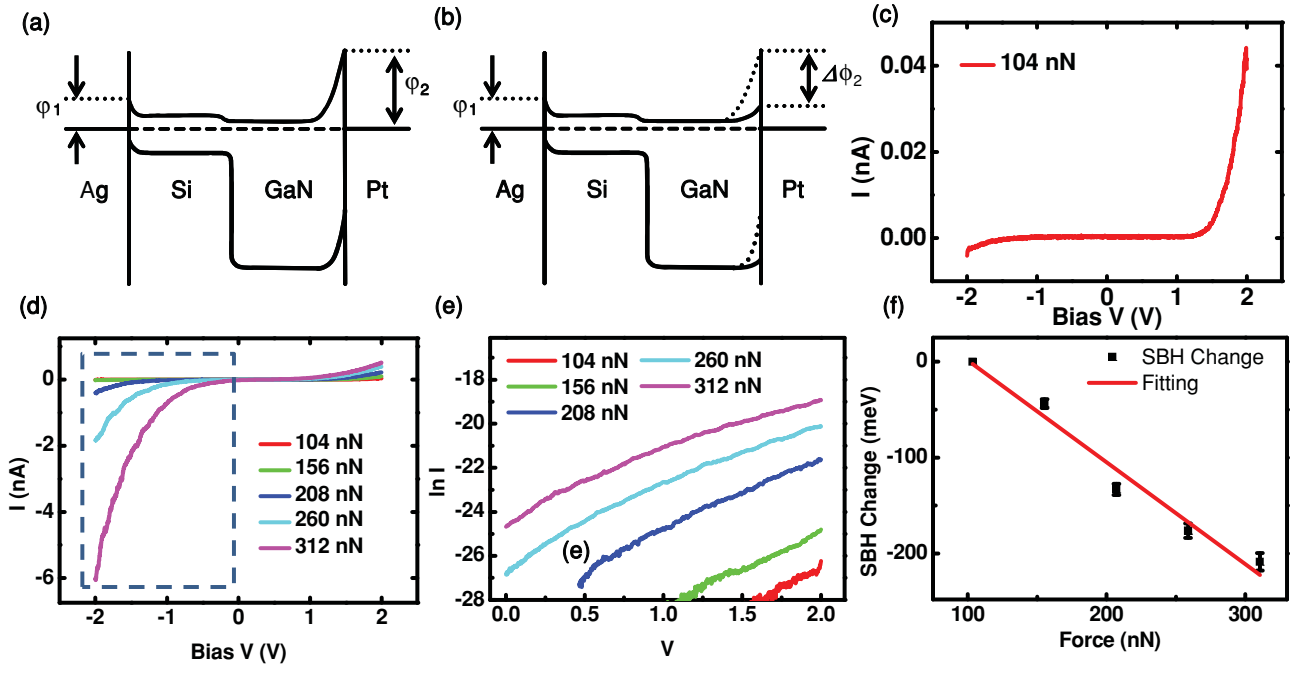

Figure 4. Energy band diagrams of the measured system to illustrate the Ag-Si Schottky barrier height between silver paste and silicon substrate (SBH, Φ_1) and the Pt-GaN Schottky barrier height (Φ_2) at the contact between the AFM tip and the GaN NW a) without and b) with a piezopotential induced by an external forced ($\triangle\Phi$ means the change in the SBH). c) Experimentally measured *I–V* characteristics under a constant transverse force of 104 nN, and d) at different forces ranging from 104 to 312 nN. e) Natural logarithm of the current vs voltage under reverse bias condition, as indicated by the dashed rectangle shown in (d). f) Calculated SBH change as a function of the applied force. The red line corresponds to the linear fitting function.

the reversely biased Ag-GaN Schottky junction, which was not affected by the induced piezopotential.

During this process, the current was also influenced by the change of contact area of the AFM tip and the GaN NW. The estimation of the influence by external force on the contact area using Derjaguin–Muller–Toporov (DMT) model[16] shows that it is negligible compared to the detected current change (details given in the Supporting Information). Furthermore, the current as a function of force was extracted from the *I*–*V* curves and analyzed. It shows significant difference in relative current change between the forward and reverse bias cases, indicating that the contact is not the dominating factor for the current change (details given in the Supporting Information). Therefore, it is fair to assume the change of the Schottky barrier height was the dominant factor in our experiment.

To quantitatively calculate the SBH change under the applied transverse force, we employed the classic Schottky models to derive the change in SBH (Φ_B) from the *I*–*V* curve. By considering the high doping concentrations (>10^{17} cm^{-3}) of the GaN NWs and that all measurements were taken at room temperature, the thermionic-emission-diffusion (TED) model and thermionic-field-emission (TFE) models are most suitable for analyzing our experimental results.[17] In the TED and TFE models, ln(*I*) is approximately proportional to $V^{1/4}$ and *V*, respectively. By plotting both ln(*I*)–$V^{1/4}$ and ln(*I*)–*V* curves (see the Supporting Information), we found that the ln(*I*)–*V* is linear, as shown in Figure 4e, indicating that the thermionic field emission process was dominant in our experiment. The reversely biased current is described in the TFE model by:

$$I = \frac{SA^{**}T}{k}\sqrt{\pi E_{00}\left[q(V-\zeta)+\frac{\phi_B}{\cosh^2(E_{00}/kT)}\right]} \times \exp\left(\frac{-\phi_B}{E_{00}\coth^2(E_{00}/kT)}\right)\exp\left(\left(\frac{1}{kT}-\frac{\tanh(E_{00}/kT)}{E_{00}}\right)qV\right) \quad (1)$$

where *S* is the area of the Schottky barrier, A^{**} is the effective Richardson constant, *T* is the temperature, *k* is Boltzmann constant, *q* is the electron charge, ζ is the distance between the Fermi energy and the bottom of the conduction band, E_{00} is the characteristic energy determined by the properties of semiconductor material:

$$E_{00} = \frac{qh}{4\pi}\sqrt{\frac{N_d}{m^*\varepsilon}} \quad (2)$$

where *h* is the Planck's constant, N_d is the doping/impurity concentration, m^* is the tunneling electron's effective mass, and ε is the dielectric constant of the NW.

Under the assumption that the square root of V is negligible compared to the exponential term, and the change in A^{**} under strain is much smaller than the change in the SBH,[17] $\Delta\Phi_B$ can be approximated using the following expression:

$$\Delta\phi_B \approx -E_{00}\coth(E_{00}/kT)\cdot\ln(I/I_0) \quad (3)$$

Based on this method (see the Supporting Information), we can plot $\Delta\Phi_B$ as a function of the applied force in Figure 4e. The linear relationship is consistent with the piezotronic model described in follows.

According to previous reports about the theory of piezotronics, the induced SBH change is linearly dependent on the piezoelectric charge density ρ_{piezo}:[15]

$$\Delta\phi_B \approx -\frac{q\ \rho_{piezo}W_{piezo}^2}{2\varepsilon} \quad (4)$$

where W_{piezo} is the width of the piezoelectric polarization charge layer. Under bending, the piezoelectric charge density depends on the NW's electrical and mechanical properties, geometry and the applied force,[18] as described in Equation 5,

$$\rho_{piezo} = F\frac{r}{I_m E}[2(1+v)e_{15}+2ve_{31}-e_{33}] \quad (5)$$

where *F* is the applied transverse force, *r* is the NW radius, I_m is the momentum, *E* is the NW's Young's modulus, *v* is the Poisson ratio and e_{ij} are the piezoelectric coefficients. From Equation 1–5, the transverse force could be linearly related to the change in the natural logarithm of the detected current $\Delta\ln(I)$,

$$F \propto \rho_{piezo} \propto \Delta\phi_B \propto \Delta\ln I \quad (6)$$

Figure 5 shows the sensitivity and response time characterized by AFM. First, a current change under certain working bias (*V* = –2 V in this case), was recorded while increasing the transverse force by a step of 16 nN. As shown in Figure 5a, the corresponding current, which is presented in semilog form, increased exponentially with applied force, consistent with the simulation and model stated above. Due to the exponential relationship between the current and force, the NW has different sensitivities in different force ranges, where the sensitivity S_l is defined as $\Delta I/\Delta F$, which is the variation in the current as the force is changed. In the lower force range (16 to 32 nN), the sensitivity is about 0.5 pA/nN; for the larger force range (64 to 80 nN), the sensitivity is about 2 pA/nN. From Figure 5a, since current change with a 16 nN force increase can be clearly differentiated, it is reasonable to claim that the force resolution is better than 16 nN.

For practical applications, a sensor with a linear relationship between the input and output is preferred. Therefore, in our case, the ln(*I*) can be used as a metric to linearly represent the applied force. From the ln(*I*)–*F* fitting line in Figure 5b, the sensitivity S_e defined to be $\Delta(\ln(I))/\Delta F$ is calculated to be 1.24 ± 0.13 ln(A)/nN by linear fitting. The response time was monitored by maximizing the sampling rate of the signal input channels of the AFM system. From Figure 5c, the current responds very well to the change in force for time intervals of 5 ms, suggesting that the sensor has no remarkable delay in response at frequency of 200 Hz. In the piezotronic transduction process, the strain induced carrier redistribution and Schottky barrier change is much faster than mechanical deformation.

In summary, we have demonstrated the transverse force sensing capability of vertically aligned GaN NWs using the piezotronic effect. By changing the Schottky barrier height, the

DOI: 10.1002/adma.201203263

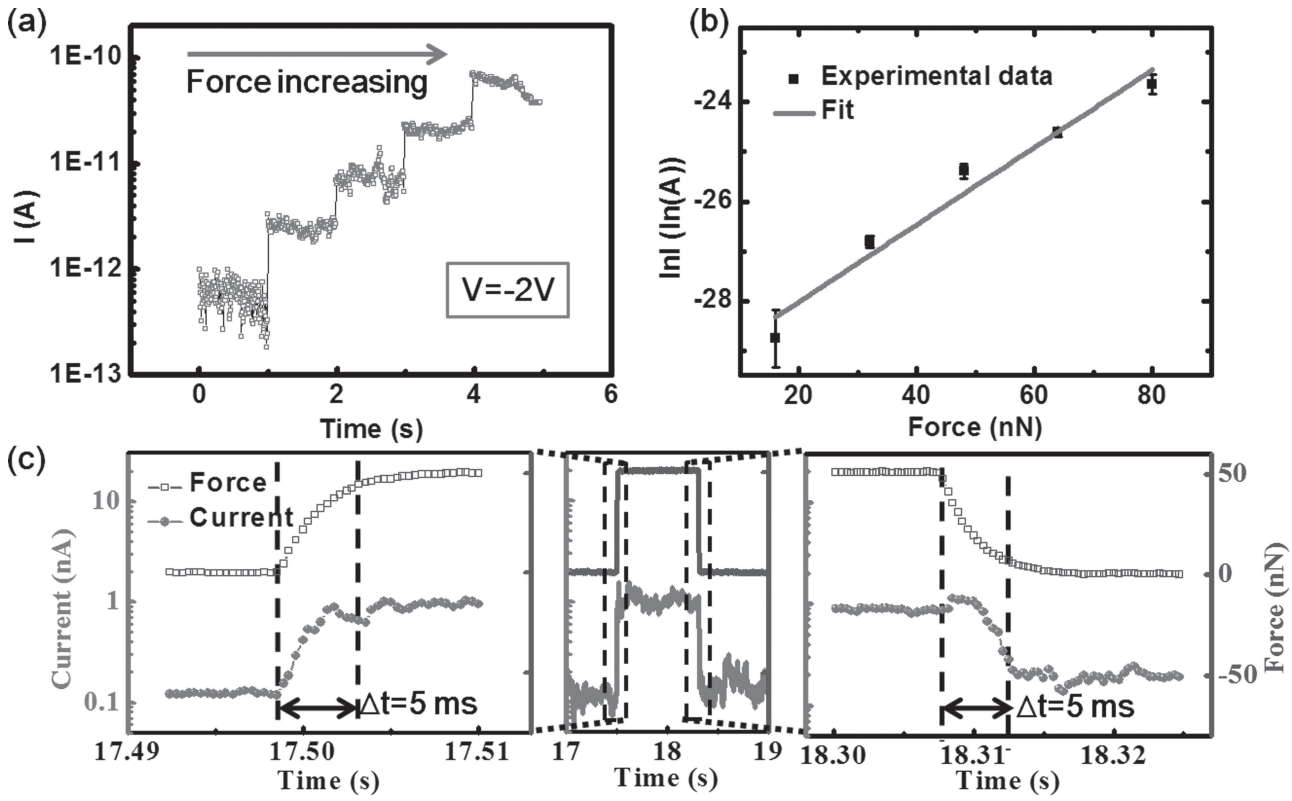

Figure 5. a) Under constant applied voltage, the current passing through the GaN NW increased step-by-step as the applied force increased. b) ln(*I*)–*F* curve demonstrating a linear relation between ln(*I*) and the applied force. c) Time response of the current change as the force changes (middle), and the response on a much shorter time scale to the increased force (left) and deceased force (right).

external transverse force could be linearly related to the natural logarithm of the current flow. The transverse force sensitivity is calculated to be 1.24 ± 0.13 ln(A)/nN, the force resolution is better than 16 nN and the response time is less than 5 ms. The nano-Newton force resolution nanowires shows the potential for piezoelectric semiconductor materials to be used as the main building block for micro/nanometer-scale sensor arrays or artificial skin.

Experimental Section

The vertically aligned GaN NWs were grown by plasma-assisted molecular beam epitaxy (PAMBE) on Si (111) wafer. Morphological and crystallographic characterizations were performed using a LEO 1530 field emission scanning electron microscope (FE-SEM) system and a JEOL-4000 transmission electron microscope (TEM).

The silicon substrate with the aligned GaN NWs was cleaved and tilted 90°. One edge of the substrate electrically connected with the AFM sample holder using silver paste, while the other edge of the substrate was characterized by a MFP-3D AFM system from Asylum Research for the *I*–*V* curves and a Dimension-3100 AFM with a Nanoscope4 controller from Bruker (Veeco) for the *V*–*t* curves. The probes used in the experiments were AC-240TM from Olympus with a Ti (5 nm)/Pt (20 nm) coating. After obtaining an image of the tilted GaN NWs, the AFM tip was positioned on top of one NW and the electrical measurements were carried out. The applied force was estimated as a function of the probe spring constant, inverse optical lever sensitivity (InvOLS) and optical lever sensed cantilever deflection. The spring constant of the probe was experimentally determined using the thermal noise method. The maximum electrical sampling rate for current detection was 8.33 kHz in the MFP-3D AFM system.

Supporting Information

Supporting Information is available from the Wiley Online Library or from the author.

Acknowledgements

Y.S.Z. and R.H. contributed equally to this work. The authors are grateful for helpful discussion from S. H. Wang and C. F. Pan. The authors are grateful for the support of the US Department of Energy, Office of Basic Energy Sciences, Division of Materials Sciences and Engineering under Award DE-FG02-07ER46394, NSF (CMMI 0403671), and the Knowledge Innovation Program of the Chinese Academy of Sciences (Grant No. KJCX2-YW-M13). The Region Rhone-Alpes contributed to financial support the exchange program of one of the authors (RH). Part of the research leading to these results has received funding from the European Community's Seventh Framework Programme (FP7/2007-2013) under grant agreement NANOFUNCTION No.257375.

Received: August 8, 2012
Revised: September 11, 2012
Published online:

[1] J. Zhou, Y. D. Gu, P. Fei, W. J. Mai, Y. F. Gao, R. S. Yang, G. Bao, Z. L. Wang, *Nano Lett.* **2008**, *8*, 3035.
[2] J. M. Wu, C. Y. Chen, Y. Zhang, K. H. Chen, Y. Yang, Y. F. Hu, J. H. He, Z. L. Wang, *ACS Nano* **2012**, *6*, 4369.
[3] J. F. Wang, M. S. Gudiksen, X. F. Duan, Y. Cui, C. M. Lieber, *Science* **2001**, *293*, 1455.
[4] a) F. Patolsky, G. F. Zheng, C. M. Lieber, *Anal. Chem.* **2006**, *78*, 4260; b) A. K. Wanekaya, W. Chen, N. V. Myung, A. Mulchandani, *Electroanalysis* **2006**, *18*, 533.
[5] Q. Wan, Q. H. Li, Y. J. Chen, T. H. Wang, X. L. He, J. P. Li, C. L. Lin, *Appl. Phys. Lett.* **2004**, *84*, 3654.
[6] Z. L. Wang, *J. Phys. Chem. Lett.* **2010**, *1*, 1388.
[7] J. Zhou, P. Fei, Y. D. Gu, W. J. Mai, Y. F. Gao, R. Yang, G. Bao, Z. L. Wang, *Nano Lett.* **2008**, *8*, 3973.
[8] W. Z. Wu, Z. L. Wang, *Nano Lett.* **2011**, *11*, 2779.
[9] a) W. Z. Wu, Y. G. Wei, Z. L. Wang, *Adv. Mater.* **2010**, *22*, 4711; b) W. Han, Y. Zhou, Y. Zhang, C. Chen, L. Lin, X. Wang, S. Wang, Z. L. Wang, *ACS Nano* **2012**, *6*, 3760.
[10] P. Fei, P. H. Yeh, J. Zhou, S. Xu, Y. F. Gao, J. H. Song, Y. D. Gu, Y. Y. Huang, Z. L. Wang, *Nano Lett.* **2009**, *9*, 3435.
[11] R. Songmuang, O. Landré, B. Daudin, *Appl. Phys. Lett.* **2007**, *91*, 251902.
[12] X. Xu, A. Potie, R. Songmuang, J. W. Lee, B. Bercu, T. Baron, B. Salem, L. Montes, *Nanotechnology* **2011**, *22*, 105704.
[13] D. R. Lide, *CRC Handbook of Chemistry and Physics*, CRC Press, Boca Raton, FL **2006**.
[14] V. Bougrov, M. E. Levinshtein, S. L. Rumyantsev, A. Zubrilov, *Properties of Advanced Semiconductor Materials: GaN, AlN, InN, BN, SiC, SiGe*, Wiley, New York **2001**, pp. 1–30.
[15] Y. Zhang, Y. Liu, Z. L. Wang, *Adv. Mater.* **2011**, *23*, 3004.
[16] a) Y. Yang, J. J. Qi, W. Guo, Y. S. Gu, Y. H. Huang, Y. Zhang, *Phys. Chem. Chem. Phys.* **2010**, *12*, 12415; b) B. V. Derjaguin, V. M. Muller, Y. P. Toporov, *Prog. Surf. Sci.* **1994**, *45*, 131.
[17] S. M. Sze, K. K. Ng, *Physics of Semiconductor Devices*, Wiley, New York **2007**, pp 134–190.
[18] Y. Gao, Z. L. Wang, *Nano Lett.* **2009**, *9*, 1103.
[19] R. Meijers, T. Richter, R. Calarco, T. Stoica, H. P. Bochem, M. Marso, H. Luth, *J. Cryst. Growth* **2006**, *289*, 381.
[20] A. Polian, M. Grimsditch, I. Grzegory, *J. Appl. Phys.* **1996**, *79*, 3343.
[21] A. D. Bykhovski, B. L. Gelmont, M. S. Shur, *J. Appl. Phys.* **1997**, *81*, 6332.
[22] A. S. Barker, M. Ilegems, *Phys. Rev. B* **1973**, *7*, 743.

Adv. Mater. **2012**,
DOI: 10.1002/adma.201203263